

# On the possible existence of an effective momentum-momentum coupling in a correlated electronic system

T. V. Trevisan,\* G. M. Monteiro,† and A. O. Caldeira

*Instituto de Física Gleb Wataghin, Universidade Estadual de Campinas, UNICAMP, 13083-859 Campinas, São Paulo, Brazil*

(Dated: December 21, 2024)

In this paper, we present a study on how to partly reincorporate the effects of localized bonding electrons on the dynamics of their itinerant counterparts in Hubbard-like Hamiltonians. This is done by relaxing the constraint that the former should be entirely frozen in the chemical bonds between the underlying lattice sites through the employment of a Born-Oppenheimer ansatz for the wavefunction of the whole electronic system. Accordingly, the latter includes itinerant as well as bonding electron coordinates. It is then argued that going beyond the adiabatic approximation, which will be properly justified in due time, we are able to show that the net effect of virtual transitions of bonding electrons between their ground and excited states is to furnish the itinerant electrons with an effective inter-electronic momentum-momentum interaction. Although we have applied these ideas to the specific case of rings, we are sure they can be easily generalized to higher dimensional systems sharing the required properties of which we have made use herein.

## I. INTRODUCTION

In Nature, the existence of strongly interacting many-body systems is the general rule rather than an exception. Everything we know of is composed of many interacting parts, and the realization that the strength of the interaction between these parts may vary within a very vast range allows us to separate length, time and energy scales, which help us establish criteria by which we can sometimes greatly simplify the dynamics of these systems. This simplification does not necessarily mean that their study can be reduced to triviality, although sometimes it really does, but we rather create a hierarchy of different levels of complexity, even having neglected a huge number of physical effects which play a minor role with respect to our aforementioned criteria.

Evidently there is a plethora of examples we could give within this modelling scheme, but let us restrict ourselves to a few of those which deal with electronic systems. The reason behind this choice is twofold. Firstly, the unquestionable relevance of the physics of electrons for the understanding of atomic and molecular structure, chemical reactions, electric and magnetic properties of solids, or, more generally, condensed matter systems, and the challenging physics of nano and mesoscopic devices. Secondly, electrons under some specific conditions are the entities we shall be addressing in this work, although we are sure our conclusions can also be extended to other interacting many-body systems.

If we focus on the low energy physics of a many-electron system, we know that the Coulomb interaction is all there is. Electron-electron, ion-ion or electron-ion interactions can all ultimately be described by Coulomb forces. Relativistic corrections include spin-orbit, spin-spin (magnetic dipole), and current-current (Breit-Darwin) interactions, all of them of electromagnetic origin, and having their importance dictated by the band structure, surface effects, and/or many other specific constraints to which the system under investigation might be subject. So, in principle, there is no secret about the basic interactions underlying a many electron system. Nevertheless, even with the advent of very fast and powerful computers, a full understanding of these systems is known to be absolutely

out of reach. In order to make use of these computational resources to get some useful information about the system, one still has to appeal to a set of ingenious numerical or simulation methods.

The computational approach to the approximate description of many electron systems is undeniably of fundamental importance, but it becomes particularly more useful when complemented with some input from simpler models from which more physical insight can be extracted. These models are the simplified versions of the realistic situations we have mentioned above, and they are meant to capture the relevant physics of the electronic system under consideration. However, it must be emphasized that, even for these simplified models, exact solutions are only rarely accessible. We shall highlight a few well-known models in what follows.

The Landau's Fermi liquid theory<sup>1</sup>, which replaces strongly interacting neutral fermions (liquid <sup>3</sup>He, for example) by weakly coupled fermionic quasi-particles with renormalized properties, can also be extended to treat charged fermions<sup>2</sup>, and becomes a paradigm for the theory of interacting electrons in metals. Although this theory was initially proposed only on phenomenological grounds, Landau himself<sup>3</sup> put forward a more microscopic justification for his own model. This together with the collective description of interactions in an electron gas constitute the basic approach for the theory of many electron systems.

Metallic crystals, on the other hand, can be modelled in two particularly simple ways<sup>4</sup>; the nearly free electron, and the tight binding models. In the former, the electrons are considered independent (except for their fermionic statistics), and subject to a very weak periodic lattice potential which can be treated by perturbation theory. The second case is the opposite extreme of the first, where the still independent electrons are strongly bound to the lattice sites, and only allowed to hop to its nearest neighbors through the overlap of the localized wave functions on each site. The hypothesis of independent electrons is supported by the strong screening effects which drastically reduces the Coulomb interaction between them, and is particularly important for very dense electronic systems. In more dilute systems the effect of the undressed Coulomb interaction is more pronounced, and in both models described

above the inter-electronic interaction can be accounted for either by the Hartree-Fock method<sup>4,5</sup>, in the weakly bound case, or by the Hubbard model in the tight-binding case (see below).

In these two cases, the lattice potential is considered static, which is enough to have a good approximate description of the electronic band structure of the system. However, to study transport phenomena<sup>6</sup>, imperfections in the periodic lattice and/or its own dynamics do really matter for the computation of response functions such as, for example, the electric conductivity of the system. Besides, lattice dynamical fluctuations are known to mediate an effective inter-electronic attractive interaction which might result in the formation of Cooper pairs<sup>7</sup>, the main charge carriers in the theory of superconductivity<sup>8</sup>. As a matter of fact, effective inter-electronic interaction is quite common in condensed matter systems and may be mediated by different excitations or components of the medium<sup>9</sup>.

In this particular contribution, we shall discuss the appearance of an effective inter-electronic interaction mediated by the electrons themselves. We will show that virtual excitations of electrons otherwise frozen in chemical bonds may induce a momentum-momentum coupling between those electrons allowed to move throughout the system subject to the lattice potential, and the inter-electronic Coulomb interaction. Although we develop our strategy for some specific models, we will later argue that the physical reasoning that led us to this finding can be extended to many other systems.

In sections II and II A we present the systems with which we shall deal in the rest of the paper, and review the basic ideas behind the application of the Hubbard model to these systems. Then, in section III, we relax the constraint that the bonding electrons must be frozen in the chemical bonds, and argue that an appropriate way to cope with the resulting physics involves going beyond the well-known Born-Oppenheimer approximation to treat the coupling between itinerant and bonding electrons. This procedure is shown to generate the desired effective momentum-momentum coupling between the itinerant electrons of the systems which is briefly analyzed in section IV.

## II. MODEL SYSTEMS: HUBBARD RINGS

In this work we study electrons in small discrete rings, i.e., electrons in  $1D$  lattices with periodic boundary conditions, when it has a finite, and small, number of sites. We denote by  $N$  the number of sites of the ring and  $a$  its lattice spacing, so that the ring's length is simply  $L = Na$ . These discrete rings are sometimes called in the literature *Hubbard rings*<sup>10</sup>, if their electronic degrees of freedom are modelled by the Hubbard model<sup>11</sup> or some extension thereof, as is the case in this work. For infinite systems of this kind ( $N \rightarrow \infty$ ) there are many different approaches to describe either approximate<sup>12</sup> or even exact solutions<sup>13</sup> for the electronic problem whereas for finite but small  $N$ , exact diagonalization is always an accessible way out of this problem.

The Hubbard model considers, on top of the self-interaction between itinerant electrons, their interaction with the effec-

tive lattice potential composed by the lattice ionic potential together with the one created by the assumed frozen cloud of bonding electrons. Since our goal here is analyze the role played by some of the latter in this specific electronic problem, we should revisit some of the essential steps taken when obtaining the Hubbard model and establish the conditions under which they will dynamically affect the model, and modify its original form.

Although we can try to make our arguments the most general possible, we think it is much more instructive to work with a specific case where our ideas can be more clearly stated. Therefore, we shall consider our ring as a closed chain of atoms which are held together by electrons in *covalent bonds*. For example, if we think of each of the ring's sites as a carbon atom, we can interpret them as prototypes of real aromatic molecules such as benzene (if one hydrogen atom is attached to each carbon atom) or the recently synthesized cyclo[18]carbon<sup>14</sup>. Besides, in so doing, we are automatically pointing to a family of systems where our results can be tested. However, contrary to real-life molecules, we impose the sites to be always static. That is because in this work we focus solely on the orbital electronic properties and, thus, we do not investigate effects related with the ionic degrees of freedom, such as the molecular vibrational levels. Another remark is that our strategy can be equally applied to infinite chains of carbon atoms which, if properly modified by the inclusion of hydrogen atoms, mimics, for example, the behavior of conducting polymers<sup>15</sup>. Let us then briefly review some useful properties of the carbon orbitals.

A neutral carbon atom has a total of six electrons, two of which are in the  $1s$  shell, strongly bound to the atom's nucleus, while the remaining four electrons are in the outermost  $2s$  and  $2p$  orbitals<sup>16</sup>. In the ring configuration (benzene molecule in particular), the  $2s$ ,  $2p_x$  and  $2p_y$  states of each carbon atom hybridize, defining three orthonormal  $sp^2$  orbitals<sup>17</sup>, whereas the  $p_z$  orbital remains unchanged. The  $sp^2$  orbitals are oriented along directions in the ring's plane that make an angle of  $2\pi/3$  between each other, and the  $p_z$  orbitals, on the other hand, are oriented perpendicularly to the ring's plane. The overlap between the  $sp^2$  orbitals of two adjacent carbon atoms, as well as the overlap between a  $sp^2$  orbital of a carbon atom and the  $s$  orbital of a hydrogen atom in the specific case of the benzene molecule, form *covalent bonds* known as  $\sigma$ -bonds. Moreover, the overlap between neighboring  $p_z$  orbitals form the so-called  $\pi$ -bonds, a weaker type of covalent bond. Briefly speaking, the  $\pi$ -bonds are weaker than the  $\sigma$ -bonds because the overlap between adjacent  $p_z$  orbitals are much smaller than that of neighboring  $sp^2$  orbitals<sup>7</sup>. Following the usual nomenclature, we hereafter denote the electrons at the  $sp^2$  orbitals by  $\sigma$ -electrons, while those occupying the  $p_z$  orbitals are called  $\pi$ -electrons.

Along this text, we focus on microscopic rings with a small number of sites,  $3 \leq N \leq 6$ , essentially because in these cases we are able to perform exact diagonalization of the Hamiltonians we study in the subsequent sections. However, the extended Hubbard model we derive in Sec. III, which is one of the most important results of this paper, holds for any number of sites  $N$  and can also be extended to a  $2D$  carbon

lattice, such as graphene. Such a generalization, however, is left for a future work, since we are here mainly interested in finite rings or 1D systems.

We choose the ring's plane coinciding with the  $xy$  plane, adopting the center of the ring as the origin of the coordinate system. In this configuration, the position of the  $j$ -th site of the ring is given by

$$\mathcal{R}_j = \frac{a}{\sqrt{2(1 - \cos(2\pi/N))}} [\cos \alpha_j \hat{x} + \sin \alpha_j \hat{y}] , \quad (1)$$

with  $j = 1, 2, \dots, N$ . Here,  $\alpha_j = 2(j-1)\pi/N$  denotes the site's angular position, and  $a$  is the lattice spacing. In analogy with the real aromatic molecules, we consider *three orbitals per ring's site*: one  $p_z$  orbital, and two  $sp^2$  orbitals. The third  $sp^2$  orbital at a given site, which binds it to another atom (such as the hydrogen atom in the case of the benzene molecule), is considered frozen, and therefore incorporated to the ring's sites, as illustrated in Fig.1. The geometric bond configuration suggests that, whatever effect there might be of the  $\sigma$ -electrons on the dynamics of the  $\pi$ -electrons, the former are much more likely to contribute only with an effective local potential to the latter.

### A. Single-band Hubbard model

The simplest model that describes the degrees of freedom of  $N_e$  itinerant and *interacting* electrons in a single orbital  $N$ -site lattice is the standard single-band Hubbard model<sup>11</sup>,

$$\hat{H}_0 = -t \sum_{j=1}^N \sum_{\sigma} \left( c_{j\sigma}^\dagger c_{j+1\sigma} + \text{h.c.} \right) + U \sum_{j=1}^N \hat{n}_{j\uparrow} \hat{n}_{j\downarrow} , \quad (2)$$

where the operator  $c_{j\sigma}^\dagger$  ( $c_{j\sigma}$ ) creates (annihilates) an electron with spin  $\sigma$  at the  $p_z$  orbital of the  $j$ -th site of the ring, and  $\hat{n}_{j\sigma} = c_{j\sigma}^\dagger c_{j\sigma}$  is the number operator. The parameter  $t$  is the

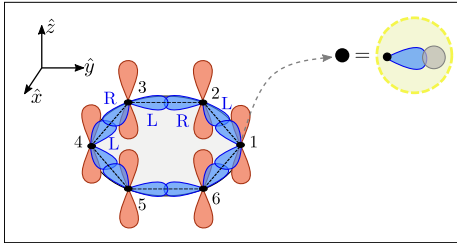


FIG. 1. **Three-band model.** Illustration of the orbital structure of the rings we consider in this work. Each of the  $N$  sites of the rings ( $N = 6$  in this figure) contains one  $p_z$  orbital and two  $sp^2$  orbitals, which we denote *left*  $sp^2$  orbital ( $L$ ) and *right*  $sp^2$  orbital ( $R$ ) according to the right-hand rule. The sites are always enumerated in ascending order in the counter-clockwise direction. The degrees of freedom of the third  $sp^2$  orbital of each site, as well as those of the valence orbitals of another atom that might bond to it, are frozen and incorporated to the ring's sites.

first-neighbor hopping<sup>11</sup> which is given by

$$t = - \int d\mathbf{r} \varphi_{i+1}^*(\mathbf{r}) \left[ -\frac{\hbar^2}{2m} \nabla^2 + V_c(\mathbf{r}) \right] \varphi_i(\mathbf{r}) , \quad (3)$$

where  $\varphi_i(\mathbf{r})$  is the Wannier wave function of an electron at the  $p_z$  orbital of site  $i$ , and  $V_c(\mathbf{r})$  is a periodic potential generated by the ions together with the core and bonding  $\sigma$ -electrons (see Fig.2). In terms of these localized wave functions, the on-site Coulomb repulsion takes the form

$$U = e^2 \int d\mathbf{r} \int d\mathbf{r}' \frac{|\varphi_i(\mathbf{r})|^2 |\varphi_i(\mathbf{r}')|^2}{|\mathbf{r} - \mathbf{r}'|} , \quad (4)$$

where  $e$  is the elementary electronic charge. If we set  $U = 0$ , Eq.(2) reduces to a purely tight-binding Hamiltonian, also known as the *Hückel Hamiltonian*.

Notice that, up to this point, we did not specify the functional forms of  $\varphi_j(\mathbf{r})$  and  $V_c(\mathbf{r})$ . The specific angular and radial dependence of  $\varphi_j(\mathbf{r})$  is important to calculate the numerical values for the parameters  $t$  and  $U$ . An estimate of these parameters is provided in<sup>18</sup> for the specific case of the prototype of benzene. Here, it is enough to keep in mind that the deeper  $V_c(\mathbf{r})$  is at the ionic positions, the larger is the tendency of the electrons to localize around those sites and, therefore, the smaller is the hopping amplitude. The bottom line is that, for now, we do not need to worry about either  $V_c(\mathbf{r})$  or  $\varphi_j(\mathbf{r})$ , since in the calculations performed in this work, except when explicitly mentioned otherwise, all physical quantities are given in units of  $t$  and/or  $U/t$ .

### B. Energy spectrum

In the case of the Hückel model (Eq.(2) with  $U = 0$ ), we can easily determine the energy levels and corresponding eigenstates of a generic ring with  $N$  sites and  $N_e$  *independent* electrons. We only need to write the electronic creation and

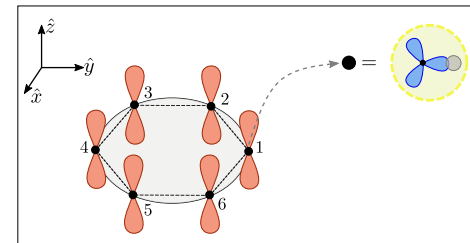


FIG. 2. **Single band model.** Illustration of the orbital structure of the rings we consider in Sec. II A. Each of the  $N$  sites of the rings ( $N = 6$  in this figure) contains *only* one  $p_z$ . The degrees of freedom of the  $sp^2$  orbitals, as well as those of the valence orbitals of another atom that might bond to it are frozen and absorbed in the ring's sites. The ring's sites are always enumerated in ascending order in the counter-clockwise direction.

annihilation operators as

$$c_{j\sigma}^\dagger = \frac{1}{\sqrt{N}} \sum_{j=1}^N e^{-i2\pi kj/N} c_{k\sigma}^\dagger, \quad (5)$$

$$c_{j\sigma} = \frac{1}{\sqrt{N}} \sum_{j=1}^N e^{i2\pi kj/N} c_{k\sigma}, \quad (6)$$

where  $c_{k\sigma}^\dagger$  ( $c_{k\sigma}$ ) creates (annihilates) an electron with spin  $\sigma$  and quasi-momentum  $k$  (with  $k = 0, 1, \dots, N-1$ ). In this way, we obtain the Hückel Hamiltonian in the *Bloch basis*

$$\hat{H}_{\text{Hückel}} = -2t \sum_{k=1}^{N-1} \sum_{\sigma=\uparrow,\downarrow} \cos\left(\frac{2\pi k}{N}\right) c_{k\sigma}^\dagger c_{k\sigma} = \sum_{k,\sigma} \varepsilon_k \hat{n}_{k,\sigma}, \quad (7)$$

where  $\hat{n}_{k\sigma} = c_{k\sigma}^\dagger c_{k\sigma}$  is the number operator in Bloch basis and

$$\varepsilon_k \equiv -2t \cos\left(\frac{2\pi k}{N}\right) \quad (8)$$

denotes the *single-particle* energy levels.

Therefore, in order to build the many-body eigenstates of energy of a ring with  $N$  sites and  $N_e$  independent electrons, among which  $N_{e\uparrow}$  have spin up and  $N_{e\downarrow}$  have spin down, we only need to fill the levels  $k$  obeying the Pauli exclusion principle. Unfortunately, such a simple picture does not hold for  $U \neq 0$ , and our only hope to determine its exact energy spectrum and corresponding eigenstates relies on numerical diagonalization.

This procedure is not a trivial task, since the dimension  $d = 2N!/(2N - N_e)!N_e!$  of the Fock space where  $\hat{H}_0$  is defined grows exponentially with the number of sites and electrons of the ring. For instance, in the case of the prototype of benzene ( $N = N_e = 6$ ),  $d = 924$ . However, it is important to note that, when dealing with large  $d$ , it is advisable to make use of the Hamiltonian's symmetry in order to rewrite it in a block-diagonal form, which reduces computational costs of the diagonalization procedure. For instance, the spin operator

$$\hat{S}_z = \sum_{j=1}^N (\hat{n}_{j\uparrow} - \hat{n}_{j\downarrow}) \quad (9)$$

commutes with  $\hat{H}_0$ , meaning that the  $z$ -component of the *total* spin of the system ( $s_z$ ) is a conserved quantity. In other words, each eigenstate of the Hubbard Hamiltonian has a well defined value of  $s_z$ , and the matrix element of  $\hat{H}_0$  between two eigenstates of  $\hat{S}_z$  with different values of  $s_z$  is identically zero. Consequently, in the basis spanned by the eigenstates of Eq.(9), the Hubbard Hamiltonian acquires a block-diagonal form, and we only need to diagonalize each block separately. Hereafter, as a matter of personal taste, we choose to work in the *site basis*, rather than in the Bloch basis. The former is spanned by  $|n_{1\uparrow}n_{1\downarrow}\dots n_{N\uparrow}n_{N\downarrow}\rangle = c_{N\downarrow}^\dagger \dots c_{1\downarrow}^\dagger c_{1\uparrow}^\dagger |0\rangle^{17}$ .

Fig. 3 shows some of the energy levels, as a function of  $U/t$ , obtained through numerical diagonalization of Eq.(2)

for rings with (a)  $N = 3$ , (b)  $N = 4$ , (c)  $N = 5$  and (d)  $N = 6$  sites. These energy spectra were calculated for the rings in the *half-filling regime*, where  $N = N_e$ . This choice is motivated by the electronic configuration of the benzene molecule, where we have a total of six  $\pi$ -electrons occupying the the six  $p_z$  orbitals of the aromatic ring. Moreover, panels (b)-(d) show just a few of the low-lying energy levels of the systems. That is because their complete energy spectrum contains a very large number of states, and including all of their representative curves in the same panel results in quite cumbersome figures.

We verified that although in some of the rings the on-site Coulomb repulsion can break some of the levels degeneracy, such as the ring with  $N = N_e = 3$ , the ground state remains degenerate (with a degeneracy four in the case of  $N = N_e = 3$ ) even for finite  $U/t$ .

### III. EXTENDED HUBBARD MODEL

The scenario we explored in Sec. II suggests a separation of energy scales in the system, as follows. Because the  $\sigma$ -electrons are localized at the ring's bonds, they could also be described approximately by another Hubbard model, but this time with a different hopping parameter,  $\tilde{t}$ , between the localized orbitals  $|sp_i^2\rangle_R$  and  $|sp_{i+1}^2\rangle_L$  (see Fig.1), and also different on-site Hubbard interaction  $\tilde{U}$ . Since these two orbitals are directed towards one another, we expect the new hopping to be larger than that involving the  $\pi$ -electrons. This means we now have a two electron - two site Hubbard model with a larger hopping describing the interacting bonding electrons. In this picture we consider bonding electrons at different bonds as distinguishable. The two lowest lying energy eigenstates of the bond will be linear combinations of

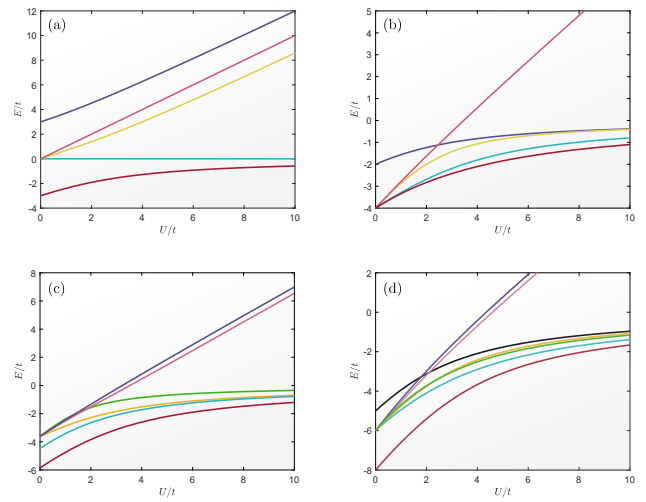


FIG. 3. **Energy spectrum of the Hubbard Hamiltonian.** The panels show the energy levels, as function of  $U/t$  for rings with (a)  $N = 3$  sites, (b)  $N = 4$  sites, (c)  $N = 5$  sites and (d)  $N = 6$  sites at the half-filling regime, i.e.,  $N = N_e$ . In the panels (b) to (d), only a few of the low-lying energy levels are plotted.

the Slater determinants of the symmetric and anti-symmetric linear combinations of the two above-mentioned neighboring orbitals. By this reasoning, it would be more costly to excite the bond to its first excited state in comparison to the characteristic energy of the  $\pi$ -electrons. In other words, the energy scale separating the ground and the first excited state of the  $\sigma$ -electrons (let's denote it by  $\Lambda$ ) is expected to be larger than the bandwidth of the  $\pi$ -electrons, which is set by a function of the hopping parameter  $t$  defined in Eq.(3). Therefore, recalling the uncertainty principle  $\Delta E \Delta t \geq \hbar/2$ , this implies that the  $\sigma$ -electrons excitations happen in a much faster time scale than that associated with the motion of the  $\pi$ -electrons around the ring.

We can thus think of two different *types* of electrons in the ring: the  $\sigma$ -electrons, which are the *fast* electrons, and the  $\pi$ -electrons which are the *slow* ones. This scenario resembles the well-known *Born-Oppenheimer approximation*, introduced in several text-books - see, for instance Ref.<sup>17</sup> - to decouple the nuclear and the electronic degrees of freedom of a molecule. Briefly speaking, due to the huge mass difference between the atomic nuclei and the electrons, the latter move around fixed positions of the former which, when allowed to move, does it in a time scale much slower than that of the electronic motion. Then, the standard Born-Oppenheimer approximation tells us that the electronic dynamics happens as if they were placed in a *static potential* generated by the nuclei in a particular frozen arrangement. For each nuclear arrangement, we are then able to diagonalize the electronic problem which, in turn, define an external potential for the nuclei themselves, and can be used to determine the molecule's vibrational levels.

The application of the same arguments for the itinerant and bonding electrons seem to be very counter-intuitive because the latter are the ones to be localized at the chemical bonds whereas the former are delocalized along the ring. Nevertheless, one should bear in mind that what must be really taken into account are the energy scales involved in the dynamics of each type of electron, and, indeed,  $\sigma$ -electrons involve higher energy than the  $\pi$ -electrons.

Here, guided by this energy scale separation, we use a perturbation approach which we call *generalized Born-Oppenheimer approximation*, in the sense that in our case the degrees of freedom of the  $\sigma$ -electrons and the  $\pi$ -electron are those to be decoupled. It is fundamental to note that, in our approximation, contrary to the standard Born-Oppenheimer approximation, the ring's sites remain static all the time. No ionic degrees of freedom are addressed in our calculations. What we are aiming at is the effect of the dynamical distortion of the periodic potential felt by the  $\pi$ -electrons due to the motion of  $\sigma$ -electrons only.

### A. Generalized Born-Oppenheimer approximation

Here, it is more convenient to return to first quantization where the *complete* Hamiltonian of a ring with  $N$  sites and  $N_e = N_e^{(\pi)} + N_e^{(\sigma)}$  electrons is given by  $\mathcal{H} = \mathcal{H}_p + \mathcal{H}_b$ ,

where

$$\mathcal{H}_p = \sum_{i=1}^{N_e^{(\pi)}} \left( \frac{\mathbf{P}_i^2}{2m} + \tilde{V}_c(\mathbf{R}_i) \right) + \frac{1}{2} \sum_{i \neq j} U(\mathbf{R}_i - \mathbf{R}_j) \quad (10)$$

describes the  $N_e^{(\pi)}$   $\pi$ -electrons, with momenta and positions denoted by  $\mathbf{R}_i$  and  $\mathbf{P}_i$ , respectively ( $i = 1, 2, \dots, N_e^{(\pi)}$ ). In this equation,  $U(\mathbf{r}, \mathbf{r}') = e^2/|\mathbf{r} - \mathbf{r}'|$  is the standard Coulomb repulsion. Moreover, the Hamiltonian

$$\begin{aligned} \mathcal{H}_b = & \sum_{\alpha=1}^{N_e^{(\sigma)}} \left( \frac{\mathbf{p}_{\alpha}^2}{2m} + \tilde{V}_c(\mathbf{r}_{\alpha}) \right) + \frac{1}{2} \sum_{\alpha \neq \beta} U(\mathbf{r}_{\alpha} - \mathbf{r}_{\beta}) \\ & + \sum_{i, \alpha} U(\mathbf{r}_{\alpha} - \mathbf{R}_i) \end{aligned} \quad (11)$$

accounts for both the degrees of freedom of  $N_e^{(\sigma)}$   $\sigma$ -electrons, with momenta and positions denoted by  $\mathbf{r}_{\alpha}$  and  $\mathbf{p}_{\alpha}$ , respectively ( $\alpha = 1, 2, \dots, N_e^{(\sigma)}$ ), and the coupling between them and the  $\pi$ -electrons. Hereafter, we reserve Roman (Greek) characters as indexes for quantities referring to  $\pi$ -electrons ( $\sigma$ -electrons). It is important to note that the periodic potential  $\tilde{V}_c(\mathbf{r})$  that appears in Eqs.(10) and (11) is not the same as  $V_c(\mathbf{r})$  defined in Eq.(3): while  $V_c(\mathbf{r})$  is generated by both the ring's sites with its core electrons, and the *frozen  $\sigma$ -electrons in the bonds*,  $\tilde{V}_c(\mathbf{r})$ , on the other hand, do not include any contribution of the  $\sigma$ -electrons. In other words, recalling our discussion in the beginning of this section,  $V_c(\mathbf{r})$  is essentially  $\tilde{V}_c(\mathbf{r})$  dressed by the static charge density in the bonds generated by the  $\sigma$ -electrons in their many-body ground state.

In this section, we denote by  $\psi(\mathbf{r}, \mathbf{R})$  the total many-body wave function of our system, where  $\mathbf{r}$  stands for the entire set of positions of the  $\sigma$ -electrons  $\{\mathbf{r}_1, \mathbf{r}_2, \dots, \mathbf{r}_{N_e^{(\sigma)}}\}$ , while  $\mathbf{R}$  denotes the set of positions of the  $\pi$ -electrons,  $\{\mathbf{R}_1, \mathbf{R}_2, \dots, \mathbf{R}_{N_e^{(\pi)}}\}$ . Our generalized Born-Oppenheimer approximation consists in assuming that the total wave function has the following separable form:

$$\psi(\mathbf{r}, \mathbf{R}) = \sum_{\nu} \phi_{\nu}(\mathbf{R}) \varphi_{\nu}(\mathbf{r}, \mathbf{R}), \quad (12)$$

where  $\phi_{\nu}(\mathbf{R})$  refers to the  $\pi$ -electrons wave functions, and  $\varphi_{\nu}(\mathbf{r}, \mathbf{R})$  denotes the  $\sigma$ -electrons wave functions for a *frozen configuration of  $\pi$ -electrons* (fixed  $\mathbf{R}$ ). The later obeys the following Schrödinger equation:

$$\mathcal{H}_b(\mathbf{R}) \varphi_{\nu}(\mathbf{r}, \mathbf{R}) = \lambda_{\nu}(\mathbf{R}) \varphi_{\nu}(\mathbf{r}, \mathbf{R}). \quad (13)$$

We emphasize that  $\mathbf{R}$  in Eq.(13) is an external parameter rather than a dynamical variable. For each  $\mathbf{R}$ , the Schrödinger equation (13) determines the  $\sigma$ -electrons eigenvalues  $\lambda_{\nu}(\mathbf{R})$  (with quantum numbers  $\nu = 0, 1, 2, \dots$ ), which, as it will shortly become clear, act as extra external potentials for the  $\pi$ -electrons. Notice that, in principle,  $\nu$  actually refers to a set  $\{n_{\alpha}\}$  where  $n_{\alpha} = 0, 1, 2, \dots$  and  $\alpha = 1, 2, \dots, 3N_e^{(\sigma)}$ . However, as we shall organize the energy levels in ascending order,

we may label  $\{n_\alpha\}$  as a sequence of integers  $\nu$ , specifying any eventual degeneracy whenever necessary.

---


$$\sum_\nu \left\{ [\mathcal{H}_p \phi_\nu(\mathbf{R}) + \lambda_\nu(\mathbf{R}) \phi_\nu(\mathbf{R})] \varphi_\nu(\mathbf{r}, \mathbf{R}) + \frac{1}{2m} \sum_{j=1}^{N_e^{(\pi)}} [\mathbf{P}_j^2 \varphi_\nu(\mathbf{r}, \mathbf{R}) + 2(\mathbf{P}_j \varphi_\nu(\mathbf{r}, \mathbf{R})) \cdot \mathbf{P}_j] \right\} \phi_\nu(\mathbf{R}) = E \sum_\nu \phi_\nu(\mathbf{R}) \varphi_\nu(\mathbf{r}, \mathbf{R}). \quad (14)$$


---

where  $\mathbf{P}_j \varphi_\nu(\mathbf{r}, \mathbf{R})$  is merely  $-i\hbar \nabla_j \varphi_\nu(\mathbf{r}, \mathbf{R})$ , the gradient of  $\varphi_\nu(\mathbf{r}, \mathbf{R})$  with respect to  $\mathbf{R}_i$  considered as a parameter in  $\varphi_\nu(\mathbf{r}, \mathbf{R})$ . Now, multiplying Eq.(14) on the left by  $\varphi_\mu^*(\mathbf{r}, \mathbf{R})$ , integrating over the  $\sigma$ -electron positions, and using the fact that  $\varphi_\mu(\mathbf{r}, \mathbf{R})$  defines an orthonormal basis, i.e.,

$$\langle \varphi_\mu | \varphi_\nu \rangle_{\mathbf{r}} = \int d\mathbf{r} \varphi_\mu^*(\mathbf{r}, \mathbf{R}) \varphi_\nu(\mathbf{r}, \mathbf{R}) = \delta_{\mu, \nu}, \quad (15)$$

we rewrite Eq.(14) as the following set of coupled equations

$$[\mathcal{H}_p + \lambda_\nu(\mathbf{R})] \phi_\nu(\mathbf{R}) + \sum_\mu \mathcal{A}_{\nu\mu} \phi_\mu(\mathbf{R}) = E \phi_\nu(\mathbf{R}). \quad (16)$$

Notice that, contrary to Eq.(13),  $\mathbf{R}$  is now a dynamical variable. Moreover, the operator  $\mathcal{A}_{\nu\mu}$  is responsible for coupling the  $\pi$ -electron wave functions with different  $\mu$  and  $\nu$ , and has the form

$$\mathcal{A}_{\nu\mu} = f_{\nu\mu}(\mathbf{R}) + \sum_{j=1}^{N_e^{(\pi)}} \mathbf{g}_{\nu\mu}^{(j)}(\mathbf{R}) \cdot \mathbf{P}_j, \quad (17)$$

with

$$f_{\nu\mu}(\mathbf{R}) \equiv -\frac{\hbar^2}{2m} \sum_{j=1}^{N_e^{(\pi)}} \langle \varphi_\nu | \nabla_j^2 \varphi_\mu \rangle_{\mathbf{r}} = -\sum_{j=1}^{N_e^{(\pi)}} \frac{\hbar^2}{2m} \int d\mathbf{r} \varphi_\nu^*(\mathbf{r}, \mathbf{R}) \nabla_j^2 \varphi_\mu(\mathbf{r}, \mathbf{R}), \quad (18)$$

and

$$\mathbf{g}_{\nu\mu}^{(j)}(\mathbf{R}) \equiv -\frac{i\hbar}{m} \langle \varphi_\nu | \nabla_j \varphi_\mu \rangle_{\mathbf{r}} = -\frac{i\hbar}{m} \int d\mathbf{r} \varphi_\nu^*(\mathbf{r}, \mathbf{R}) \nabla_j \varphi_\mu(\mathbf{r}, \mathbf{R}). \quad (19)$$

In order to develop a more intuitive picture of the meaning of Eqs.(13) and (16) let us make a symbolic sketch of  $\lambda_\nu(\mathbf{R})$ . Fig. 4(a) shows an illustration of three of these eigenvalues as if they were a function of a scalar variable, in analogy with the standard Born-Oppenheimer approximation, to which we are more used. In reality, of course,  $\lambda_\nu(\mathbf{R})$  defines a hypersurface in the space configuration of the  $\pi$ -electrons. Hereafter,

Substituting the ansatz (12) into the full time-independent Schrödinger equation  $\mathcal{H}\psi = E\psi$  and using Eq.(13), we find that the  $\pi$ -electrons wave function must obey

$$\mathcal{H}_0 \phi_{0,n}(\mathbf{R}) + \mathcal{A}_{01} \phi_{1,n}(\mathbf{R}) = E_n \phi_{0,n}(\mathbf{R}), \quad (20)$$

$$\mathcal{H}_1 \phi_{1,n}(\mathbf{R}) + \mathcal{A}_{10} \phi_{0,n}(\mathbf{R}) = E_n \phi_{1,n}(\mathbf{R}), \quad (21)$$

where the index  $n$  labels the quantum numbers which characterizes the system's energy levels. Besides, we define  $\mathcal{H}_0 \equiv \mathcal{H}_p + \lambda_0(\mathbf{R}) + \mathcal{A}_{00}$  and  $\mathcal{H}_1 \equiv \mathcal{H}_p + \lambda_1(\mathbf{R}) + \mathcal{A}_{11}$ . We emphasize that in the language of second quantization,  $\mathcal{H}_0$  is a single-band Hubbard Hamiltonian with a renormalized hopping amplitude  $t_0$ . Similarly,  $\mathcal{H}_1$  is a Hubbard Hamiltonian with another hopping parameter  $t_1$ .

In the limit that  $\lambda_0(\mathbf{R})$  and  $\lambda_1(\mathbf{R})$  are energetically too far apart,  $(\Lambda_{1,0}(\mathbf{R}) \equiv \lambda_1(\mathbf{R}) - \lambda_0(\mathbf{R}) \gg t_0, U)$ ,  $\mathcal{A}_{\nu\mu}$  becomes negligible. Consequently, Eqs.(20) and (21) decouple and the system's energy levels are just the set composed by the union of the eigenvalues of  $\mathcal{H}_0$  and  $\mathcal{H}_1$ , illustrated by the horizontal black lines in Fig. 4(b). Notice that, in this limit, the low-lying energy states of the system are those of  $\mathcal{H}_0$ , which means that the  $\pi$ -electrons move along the ring as if the  $\sigma$ -electrons were

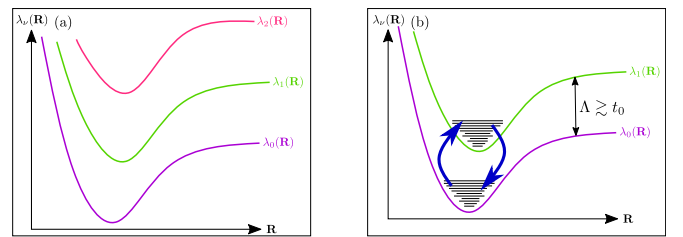


FIG. 4. Energy "surfaces" of the  $\sigma$ -electrons. Illustration of the energy levels of the  $\sigma$ -electrons as function of the  $\pi$ -electrons configuration  $\lambda_\nu(\mathbf{R})$  as if they were a function of a scalar variable, in analogy to the simpler standard Born-Oppenheimer approximation. Panel (a) represents the first three low-lying  $\lambda_\nu(\mathbf{R})$ . Panel (b) focus only on the first two  $\sigma$ -electrons energy levels. In each one of them, the  $\pi$ -electron Hubbard spectrum is represented by the horizontal black lines. The blue arrows indicates virtual excitations that may occur in the system if the energy separation ( $\Lambda$ ) between the two  $\sigma$ -electron surfaces is comparable with the  $\pi$ -electrons band width.

actually frozen in their ground state  $\lambda_0(\mathbf{R})$ , recovering the standard Hubbard model we described in Sec.II A. The interesting limit is when  $\Lambda_{1,0}(\mathbf{R})$  is still larger than  $t_0$ , but they are of the *same order* ( $\Lambda_{1,0}(\mathbf{R}) \gtrsim t_0, U$ ). This is exactly the case of our rings, as we have shown elsewhere<sup>18</sup>, and in this limit  $\mathcal{A}_{\nu\mu}$  cannot be neglected. Actually, this operator mixes the eigenstates of  $\mathcal{H}_0$  and  $\mathcal{H}_1$ . Let's explore this scenario in more details in the next paragraphs.

Isolating  $\phi_{1,n}(\mathbf{R})$  in Eq.(21) and substituting it in Eq.(20), we obtain an effective Schrödinger equation for  $\phi_{0,n}(\mathbf{R})$ ,

$$\left[ \mathcal{H}_0 + \mathcal{A}_{01} (E_n - \mathcal{H}_1)^{-1} \mathcal{A}_{10} \right] \phi_{0,n}(\mathbf{R}) = E_n \phi_{0,n}(\mathbf{R}) . \quad (22)$$

Note that

$$\mathcal{W}_{eff}(\mathbf{P}, \mathbf{R}) \equiv \mathcal{A}_{01} (E_n - \mathcal{H}_1)^{-1} \mathcal{A}_{10} , \quad (23)$$

which in general depends on both momenta and positions, defines an *effective interaction* between the  $\pi$ -electrons, which carries information about the virtual excitations of the  $\sigma$ -electrons. Moreover, Eq.(22) is a self-consistent equation, since the potential defined in Eq.(23) itself depends on the energy levels  $E_n$  we want to calculate. Fortunately, this is a typical problem which can be approached by the well-known *Wigner-Brillouin perturbation theory*<sup>17</sup>.

Let us denote by  $\zeta_{0,n}(\mathbf{R})$  and  $\varepsilon_n^{(0)}$  ( $\zeta_{1,n}(\mathbf{R})$  and  $\varepsilon_n^{(1)}$ ) the eigenstates and corresponding eigenvalues of the Hubbard-like Hamiltonian  $\mathcal{H}_0$  ( $\mathcal{H}_1$ ). Both  $\zeta_{0,n}(\mathbf{R})$  and  $\zeta_{1,n}(\mathbf{R})$  span an orthonormal basis, i.e.

$$\sum_n |\zeta_{\nu,n}\rangle \langle \zeta_{\nu,n}| = \mathbb{1} , \quad (24)$$

$$\langle \zeta_{\nu,n} | \zeta_{\nu,m} \rangle = \int d\mathbf{R} \zeta_{\nu,n}^*(\mathbf{R}) \zeta_{\nu,m}(\mathbf{R}) = \delta_{n,m} , \quad (25)$$

with  $\nu = 0, 1$  and  $\langle \zeta_{0,n} | \zeta_{1,m} \rangle \neq \delta_{m,n}$ . Wigner-Brillouin perturbation theory tells us that  $\phi_{0,n}(\mathbf{R})$  and  $\zeta_{0,n}(\mathbf{R})$ , as well as  $E_n$  and  $\varepsilon_n$  are related through

$$\begin{aligned} \phi_{0,n}(\mathbf{R}) &= \zeta_{0,n}(\mathbf{R}) + \sum_{m \neq n} \frac{\langle \zeta_{0,m} | \mathcal{W}_{eff} | \zeta_{0,n} \rangle}{E_n - \varepsilon_m^{(0)}} \zeta_{0,m}(\mathbf{R}) \\ &+ \mathcal{O}(\mathcal{W}_{eff}^2) , \end{aligned} \quad (26)$$

$$E_n = \varepsilon_n + \langle \zeta_{0,n} | \mathcal{W}_{eff} | \zeta_{0,n} \rangle + \mathcal{O}(\mathcal{W}_{eff}^2) , \quad (27)$$

with

$$\langle \zeta_{0,m} | \mathcal{W}_{eff} | \zeta_{0,n} \rangle = \int d\mathbf{R} \zeta_{0,m}^*(\mathbf{R}) \mathcal{W}_{eff}(\mathbf{P}, \mathbf{R}) \zeta_{0,n}(\mathbf{R}) \quad (28)$$

being the matrix element of the effective interaction (23) in the basis spanned by the  $\zeta_{0,n}(\mathbf{R})$  states.

In zeroth order perturbation theory for the energy ( $E_n \approx \varepsilon_n^{(0)}$ ), and neglecting quadratic or higher orders of  $\mathcal{W}_{eff}$  in

the perturbation expression for the eigenstates, we obtain

$$\begin{aligned} \phi_{0,n}(\mathbf{R}) &\approx \zeta_{0,n}(\mathbf{R}) + \sum_{m \neq n} \frac{1}{\varepsilon_n^{(0)} - \varepsilon_m^{(0)}} \\ &\times \left\langle \zeta_{0,m} \left| \mathcal{A}_{01} \left( \varepsilon_n^{(0)} - \mathcal{H}_1 \right)^{-1} \mathcal{A}_{10} \right| \zeta_{0,n} \right\rangle \zeta_{0,m}(\mathbf{R}) , \end{aligned} \quad (29)$$

from which it is clear that the matrix element defined in Eq.(28) simplifies to

$$\langle \zeta_{0,m} | \mathcal{W}_{eff} | \zeta_{0,n} \rangle \approx -\frac{1}{\Lambda} \langle \zeta_{0,m} | \mathcal{A}_{01} \mathcal{O}_n \mathcal{A}_{10} | \zeta_{0,n} \rangle , \quad (30)$$

where  $\mathcal{O}_n$  is a complicated many-body operator defined as

$$\mathcal{O}_n \equiv \sum_m \left( 1 - \frac{\varepsilon_n^{(0)} - \varepsilon_m^{(0)}}{\Lambda} \right)^{-1} |\zeta_{1,m}\rangle \langle \zeta_{1,m}| . \quad (31)$$

To derive Eqs.(30) and (31), we use the closure relation in Eq.(24) to rewrite  $\varepsilon_n^{(0)} - \mathcal{H}_1$  in Eq.(29) as

$$\begin{aligned} \varepsilon_n^{(0)} \mathbb{1} - \sum_m \varepsilon_m^{(1)} |\zeta_{1,m}\rangle \langle \zeta_{1,m}| &= \\ \sum_m \left( \varepsilon_n^{(0)} - \varepsilon_m^{(1)} \right) |\zeta_{1,m}\rangle \langle \zeta_{1,m}| . \end{aligned} \quad (32)$$

Besides, we approximate the energy levels of  $\mathcal{H}_1$  as those of  $\mathcal{H}_0$  displaced by the energy separation between the two  $\sigma$ -electrons energy surfaces, i.e.

$$\varepsilon_m^{(1)} \approx \varepsilon_m^{(0)} + \Lambda_{1,0}(\mathbf{R}) . \quad (33)$$

Recall that we previously define  $\Lambda_{1,0}(\mathbf{R}) \equiv \lambda_1(\mathbf{R}) - \lambda_0(\mathbf{R})$ . Interestingly, in<sup>18</sup> it is shown that such energy spacing between the  $\sigma$ -electrons energy surface depends weakly on  $\mathbf{R}$ , so it is reasonable to approximate it by a constant,  $\Lambda_{1,0}(\mathbf{R}) \approx \Lambda > 0$ , consistently with the notation we have been using since the beginning of this section.

Unfortunately, even after the aforementioned approximations, the effective interaction is still very complicated to be evaluated because of the infinite sum involving the projectors in Eq.(31). Thus, to proceed further, we need to establish new simplifying hypotheses, and approximations, which are described in detail in the next subsection.

## B. Effective interaction in first quantization

The first thing we need to do is return to the expression of  $\mathcal{A}_{\nu\mu}$  defined in Eqs.(17)-(19) and find an approximate expression for it. Let us start studying  $\mathbf{g}_{\nu\mu}^{(j)}(\mathbf{R})$ .

Note that taking the gradient of Eq.(13) with respect to the position of the  $j$ -th  $\pi$ -electron, multiplying the result on the left by  $\varphi_{\nu}^*(\mathbf{r}, \mathbf{R})$ , and integrating over the positions of the  $\sigma$ -electrons, we obtain

$$\int d\mathbf{r} \varphi_\nu^*(\mathbf{r}, \mathbf{R}) \nabla_j \varphi_\mu(\mathbf{r}, \mathbf{R}) = \frac{1}{\lambda_\mu(\mathbf{R}) - \lambda_\nu(\mathbf{R})} \int d\mathbf{r} \varphi_\nu^*(\mathbf{r}, \mathbf{R}) (\nabla_j \mathcal{H}_b) \varphi_\mu(\mathbf{r}, \mathbf{R}) . \quad (34)$$

Recall that  $\mathbf{R}$  is merely an external parameter for  $\mathcal{H}_b$ , and it appears only in the Coulomb repulsion term (see Eq.(11)). Therefore, it follows that

$$\nabla_j \mathcal{H}_b(\mathbf{R}) = e^2 \sum_{\alpha=1}^{N_e^{(\sigma)}} \frac{\mathbf{r}_\alpha - \mathbf{R}_j}{|\mathbf{r}_\alpha - \mathbf{R}_j|^3} . \quad (35)$$

Our task now is to evaluate the integral over the positions

of the  $\sigma$ -electrons. Since we have a term  $|\mathbf{r}_\alpha - \mathbf{R}_j|^3$  in the denominator of the integrand, the  $\sigma$ -electrons which are closer to the  $j$ -th  $\pi$ -electron are those which give the largest contribution to the right-hand side of Eq.(34). Furthermore, as discussed in Sec. II, we have two  $\sigma$ -electrons per bond. Consequently, for each  $\pi$ -electron localized at a given ring site, there are four nearest neighbors  $\sigma$ -electrons, here labeled by 1 to 4 for simplicity, that dominates the sum in Eq.(35), which we can approximate as

$$\begin{aligned} \int d\mathbf{r} \varphi_\nu^*(\mathbf{r}, \mathbf{R}) (\nabla_j \mathcal{H}_b) \varphi_\mu(\mathbf{r}, \mathbf{R}) &\approx e^2 \hat{\mathbf{d}}_j^{(L)} \int d\mathbf{r} \varphi_\nu^*(\mathbf{r}, \mathbf{R}) \left( \frac{1}{|\mathbf{r}_1 - \mathbf{R}_j|^2} + \frac{1}{|\mathbf{r}_2 - \mathbf{R}_j|^2} \right) \varphi_\mu(\mathbf{r}, \mathbf{R}) + \\ &+ e^2 \hat{\mathbf{d}}_j^{(R)} \int d\mathbf{r} \varphi_\nu^*(\mathbf{r}, \mathbf{R}) \left( \frac{1}{|\mathbf{r}_3 - \mathbf{R}_j|^2} + \frac{1}{|\mathbf{r}_4 - \mathbf{R}_j|^2} \right) \varphi_\mu(\mathbf{r}, \mathbf{R}) , \end{aligned} \quad (36)$$

where we have defined

$$\hat{\mathbf{d}}_j^{(R)} \equiv \frac{1}{a} (\mathcal{R}_{j+1} - \mathcal{R}_j) \quad (37)$$

as the versor in the direction of the *right*  $\sigma$ -bond, between the sites  $j$  and  $j+1$ . Recall that  $\mathcal{R}_j$  is the position of site  $j$  defined in Eq.(1). On the other hand,  $\hat{\mathbf{d}}_j^{(L)}$  denotes the versor in the direction of the *left*  $\sigma$ -bond and it is related with Eq.(37) through  $\hat{\mathbf{d}}_j^{(L)} = -\hat{\mathbf{d}}_{j-1}^{(R)}$ .

Concerning the remaining integrals on the right-hand side of Eq.(36), if we had  $|\mathbf{r}_\alpha - \mathbf{R}_j|$  in the denominator, they would be of the order of the on-site Coulomb repulsion between  $\pi$ -electrons and  $\sigma$ -electrons,  $\tilde{U}$ , which we assume to be of the same order as the on-site repulsion ( $U$ ) between the  $\pi$ -electrons. Moreover, it follows from the discussion in the previous paragraph that  $|\mathbf{r}_\alpha - \mathbf{R}_j|$  is of the order of the lattice spacing  $a$ . Consequently, we can roughly estimate for  $\mu \neq \nu = 0, 1$ , which is our particular case,

$$e^2 \int d\mathbf{r} \varphi_\nu^*(\mathbf{r}, \mathbf{R}) \frac{1}{|\mathbf{r}_1 - \mathbf{R}_j|^2} \varphi_\mu(\mathbf{r}, \mathbf{R}) \sim \frac{\tilde{U}}{a} , \quad (38)$$

and similarly for the other integrals involving  $\mathbf{r}_2$ ,  $\mathbf{r}_3$  and  $\mathbf{r}_4$ . Therefore, Eq.(36) results in

$$\begin{aligned} \int d\mathbf{r} \varphi_\nu^*(\mathbf{r}, \mathbf{R}) (\nabla_j \mathcal{H}_b) \varphi_\mu(\mathbf{r}, \mathbf{R}) &\approx \\ &\approx 2 \frac{\tilde{U}}{a} \left( \hat{\mathbf{d}}_j^{(R)} - \hat{\mathbf{d}}_{j-1}^{(R)} \right) = 2 \frac{U}{a} \hat{\mathbf{n}}_j . \end{aligned} \quad (39)$$

Here  $\hat{\mathbf{n}}_j$  is the versor in the direction of the position of the site at which the  $\pi$ -electron is localized, but pointing inwards. Notice that we have assumed  $|\hat{\mathbf{d}}_j^{(R)} - \hat{\mathbf{d}}_{j-1}^{(R)}| \tilde{U} = U$ .

Substituting Eq.(39) into Eq.(34) and comparing it with (19) we readily identify

$$\mathbf{g}_{\nu\mu}^{(j)}(\mathbf{R}) \approx -\frac{i\hbar}{am} \frac{2U}{\lambda_\mu(\mathbf{R}) - \lambda_\nu(\mathbf{R})} \left( \hat{\mathbf{d}}_j^{(R)} - \hat{\mathbf{d}}_{j-1}^{(R)} \right) . \quad (40)$$

Regarding  $f_{\nu\mu}(\mathbf{R})$ , we have neglected it since this term is of  $\mathcal{O}(U^2/\Lambda^2)$  and does not involve the  $\pi$ -electrons momenta and, therefore, when included in Eq.(23) gives rise, in first order perturbation theory, to a one-body term that can be incorporated in the hopping parameter. Therefore, from Eq.(40), and as in the previous section, assuming  $\lambda_1(\mathbf{R}) - \lambda_0(\mathbf{R}) \approx \Lambda > 0$  (constant), we can approximate  $\mathcal{A}_{01}$  and  $\mathcal{A}_{10}$  by the simple one-body operators

$$\mathcal{A}_{01} \approx -\frac{2i\hbar U}{ma\Lambda} \sum_{j=1}^{N_e^{(\sigma)}} \hat{\mathbf{n}}_j \cdot \mathbf{P}_j , \quad (41)$$

$$\mathcal{A}_{10} \approx \frac{2i\hbar U}{ma\Lambda} \sum_{j=1}^{N_e^{(\sigma)}} \hat{\mathbf{n}}_j \cdot \mathbf{P}_j . \quad (42)$$

At this point, we have almost everything we need to derive a simplified expression for  $\mathcal{W}_{eff}$  in first quantization. All we need now is return to Eq.(31), and analyze it more carefully. If  $\mathcal{O}_n$  were a constant, it would generate a  $\mathcal{W}_{eff}$  which would be just a product of two one-body operators, instead of a true two-body operator. However, the very form of  $\mathcal{O}_n$ , if written in coordinate representation, induces us to assume it is a non-separable function of the generalized coordinates  $\mathbf{R}$  and  $\mathbf{R}'$ . Therefore, the simplest assumption we can make about Eq.(31) is to neglect contributions from three, four-body interactions and so on, that is, it only has a two-body component

which can correlate the momentum operators that appear in Eqs.(41) and (42). In this case, we can write

$$\mathcal{W}_{eff} \approx -\frac{1}{\Lambda^3} \left( \frac{2\hbar U}{ma} \right)^2 \sum_{i,j=1}^{N_e} \mathbf{P}_i \cdot \hat{\mathbf{n}}_i \mathcal{O}(\mathbf{R}_i, \mathbf{R}_j) \hat{\mathbf{n}}_j \cdot \mathbf{P}_j . \quad (43)$$

Note that since  $\hat{\mathbf{n}}_j$  is a simple versor rather than an operator, we can freely interchange it with the momentum operator, i.e.  $\hat{\mathbf{n}}_j \cdot \mathbf{P}_j = \mathbf{P}_j \cdot \hat{\mathbf{n}}_j$ , and define a tensor

$$\overleftrightarrow{T}(\mathbf{R}_i, \mathbf{R}_j) \equiv \hat{\mathbf{n}}_i \mathcal{O}(\mathbf{R}_i, \mathbf{R}_j) \hat{\mathbf{n}}_j , \quad (44)$$

which encodes the information about the ring's  $\sigma$ -bonds orientation through the versors  $\hat{\mathbf{n}}_i$ .

An effective attractive momentum-momentum interaction with a form similar to that of Eq.(43) appeared in the literature some decades ago, when Bohm and Pines wrote the seminal series of papers about the electron gas<sup>20-22</sup>. They were able to show that there is an effective inter-electronic potential mediated by plasmons (longitudinal plasma fluctuations), which they called a *residual interaction*<sup>22</sup>. However, they argued that such an interaction is negligible because of the screening effects in a dense electron gas. In our case, on the other hand, since we are dealing with a few body system, screening effects are not strong enough to suppress this kind of interaction.

Only for the sake of completeness, it is worth mentioning that in<sup>20</sup> they also described the effective inter-electronic interaction mediated by transverse electromagnetic radiation in the electronic medium. This also results in a momentum-momentum interaction, that they recognized as a Biot-Savart interaction. The latter is basically unscreened, and is a relativistic correction of the order of  $(v/c)^2$  to the inter-electronic interaction. Incidentally, in classical electrodynamics, this same interaction is also described by the so-called Breit-Darwin (or current-current) interaction<sup>23</sup>.

### C. Effective interaction in second quantization

In the previous section we show that virtual excitations of the  $\sigma$ -electrons mediate an effective momentum-momentum attraction between the  $\pi$ -electrons, which, in first quantization, is given by Eq.(43). Here, we derive its expression in the language of second quantization. By adding the second-quantized  $\mathcal{W}_{eff}$  to Eq.(2), we derive an extended Hubbard Hamiltonian for the degrees of freedom of the  $\pi$ -electrons alone, but which takes into account the effects of the  $\sigma$ -electrons in their dynamics. It is important to note that in this section  $\mathbf{r}$  no longer denotes the set of positions of the  $\sigma$ -electrons, but rather a generic position in space.

Since  $\mathcal{W}_{eff}$  in Eq.(43) is a two-body operator, the standard procedure to determine its second-quantized expression is<sup>5,17</sup>

$$\hat{\mathcal{W}}_{eff} = \frac{1}{2} \sum_{\sigma, \sigma'} \int \int d\mathbf{r} d\mathbf{r}' \hat{\psi}_\sigma^\dagger(\mathbf{r}) \hat{\psi}_{\sigma'}^\dagger(\mathbf{r}') \mathbf{P} \cdot \overleftrightarrow{T}(\mathbf{r}, \mathbf{r}') \cdot \mathbf{P}' \hat{\psi}_{\sigma'}(\mathbf{r}') \hat{\psi}_\sigma(\mathbf{r}) , \quad (45)$$

where, in coordinate representation,  $\mathbf{P} = -i\hbar\nabla$  and  $\mathbf{P}' = -i\hbar\nabla'$ , with  $\nabla'$  denoting the gradient with respect to  $\mathbf{r}'$ . Besides,  $\hat{\psi}_\sigma^\dagger(\mathbf{r})$  ( $\hat{\psi}_\sigma(\mathbf{r})$ ) is the field operator that creates (annihilates) an electron with spin  $\sigma$  at the position  $\mathbf{r}$ . Since we are deriving an effective model for the  $\pi$ -electrons alone, such a field operator is defined only in terms of the Wannier wave functions of the  $p_z$  orbitals ( $\varphi_{j\sigma}(\mathbf{r})$ ), as  $\hat{\psi}_\sigma(\mathbf{r}) = \sum_{i,\sigma} \varphi_{i\sigma}(\mathbf{r}) c_{i\sigma}$ , where  $c_{i\sigma}$  annihilates an electron with spin  $\sigma$  at the site  $i$ . Here the reader should be warned not to confuse  $\varphi_j(\mathbf{r})$  with the  $\sigma$ -electrons wave functions  $\varphi_\nu(\mathbf{r}, \mathbf{R})$  we

defined in Sec. III A.

Substituting the expression for  $\hat{\psi}_\sigma(\mathbf{r})$  in terms of  $c_{i\sigma}$  into Eq.(45) we find the second-quantized effective interaction in the *site basis*,

$$\hat{\mathcal{W}}_{eff} = -\frac{1}{2\Lambda^3} \left( \frac{2\hbar U}{ma} \right)^2 \sum_{i,j,k,l=1}^N \sum_{\sigma, \sigma'} w_{ijkl} c_{i\sigma}^\dagger c_{j\sigma'}^\dagger c_{k\sigma'} c_{l\sigma} , \quad (46)$$

where  $w_{ijkl}$  is the matrix element

$$w_{ijkl} \equiv \left\langle ij \left| \mathbf{P} \cdot \overleftrightarrow{T} \cdot \mathbf{P}' \right| lk \right\rangle = -\hbar^2 \int \int d\mathbf{r} d\mathbf{r}' \varphi_i^*(\mathbf{r}) \varphi_j^*(\mathbf{r}') \nabla \cdot \overleftrightarrow{T}(\mathbf{r}, \mathbf{r}') \cdot \nabla' \varphi_k(\mathbf{r}') \varphi_l(\mathbf{r}) , \quad (47)$$

which we study in detail henceforth.

To start with, we apply the closure identity,

$$\mathbb{1} = \sum_{i,j=1}^N |ij\rangle \langle ij| , \quad (48)$$

between the momentum operators and the tensor  $\overleftrightarrow{T}$ , which gives us

$$w_{ijkl} = \sum_{i_1, i_2} \sum_{j_1, j_2} \langle ij | \mathbf{P} | i_1 i_2 \rangle \cdot \langle i_1 i_2 | \overleftrightarrow{T} | j_1 j_2 \rangle \cdot \langle j_1 j_2 | \mathbf{P}' | lk \rangle. \quad (49)$$

Note that  $\mathbf{P}$  acts only on the *first* entry of a ket  $|ij\rangle$ , i.e.

$$\langle \mathbf{r} \mathbf{r}' | \mathbf{P} | ij \rangle = \langle \mathbf{r} | \mathbf{P} | i \rangle \langle \mathbf{r}' | j \rangle. \quad (50)$$

Similarly,  $\mathbf{P}'$  acts only on the second entry of  $|ij\rangle$ . Therefore

$$\langle ij | \mathbf{P} | i_1 i_2 \rangle = \langle i | \mathbf{P} | i_1 \rangle \langle j | i_2 \rangle = \langle i | \mathbf{P} | i_1 \rangle \delta_{j, i_2}, \quad (51)$$

$$\langle j_1 j_2 | \mathbf{P}' | lk \rangle = \langle j_2 | \mathbf{P}' | k \rangle \langle j_1 | l \rangle = \langle j_2 | \mathbf{P}' | k \rangle \delta_{j_1, l}, \quad (52)$$

and, as a consequence of the orthonormality of the Wannier

wave functions, Eq.(49) becomes

$$w_{ijkl} = \sum_{i_1, j_2=1}^N \sum \langle i | \mathbf{P} | i_1 \rangle \cdot \langle i_1 j | \overleftrightarrow{T} | l j_2 \rangle \cdot \langle j_2 | \mathbf{P}' | k \rangle. \quad (53)$$

Now, consistently with the standard approximations used to derive the single-band Hubbard Hamiltonian<sup>11</sup>, we can show (see Appendix ) that the momentum matrices elements appearing in Eq.(53) can be approximated by a term connecting only nearest neighbor sites,

$$\langle i | \mathbf{P} | j \rangle \approx \frac{imt}{\hbar} (\mathcal{R}_i - \mathcal{R}_j) \delta_{j, i \pm 1}. \quad (54)$$

Recall that  $\mathcal{R}_i$  is the position of the  $i$ -th site of the ring given by Eq.(1),  $t$  is the hopping parameter between two neighboring  $p_z$  orbital, and  $m$  is the electron mass. Therefore, substituting Eq.(54) into Eq.(53) we obtain four contributions for  $w_{ijkl}$ :

$$\begin{aligned} w_{ijkl} \approx & - \left( \frac{mt}{\hbar} \right)^2 \times \\ & \times \left[ (\mathcal{R}_i - \mathcal{R}_{i+1}) \cdot \langle i+1 | \overleftrightarrow{T} | l \ k+1 \rangle \cdot (\mathcal{R}_{k+1} - \mathcal{R}_k) + (\mathcal{R}_i - \mathcal{R}_{i+1}) \cdot \langle i+1 | \overleftrightarrow{T} | l \ k-1 \rangle \cdot (\mathcal{R}_{k-1} - \mathcal{R}_k) \right. \\ & \left. + (\mathcal{R}_i - \mathcal{R}_{i-1}) \cdot \langle i-1 | \overleftrightarrow{T} | l \ k+1 \rangle \cdot (\mathcal{R}_{k+1} - \mathcal{R}_k) + (\mathcal{R}_i - \mathcal{R}_{i-1}) \cdot \langle i-1 | \overleftrightarrow{T} | l \ k-1 \rangle \cdot (\mathcal{R}_{k-1} - \mathcal{R}_k) \right]. \end{aligned} \quad (55)$$

Concerning the matrix element of the tensor  $\overleftrightarrow{T}$ , we assume, as it is done with the Coulomb repulsion matrix elements in the standard Hubbard model<sup>11</sup>, that its leading contributions come from the on-site terms. Mathematically, this means

$$\langle ij | \overleftrightarrow{T} | lk \rangle \approx \overleftrightarrow{T}_i \delta_{j,i} \delta_{k,i} \delta_{l,i}, \quad (56)$$

where we define  $\overleftrightarrow{T}_i \equiv \langle ii | \overleftrightarrow{T} | ii \rangle$ . As it will soon become clearer (see Eq.(58)),  $\overleftrightarrow{T}_i$  depends on the specific  $i$ -th site of the ring.

Returning to the definition of  $\overleftrightarrow{T}$  in Eq.(44), we can write

$$\overleftrightarrow{T}_i = \int \int d\mathbf{r} d\mathbf{r}' \varphi_i^*(\mathbf{r}) \varphi_i^*(\mathbf{r}') \hat{\mathbf{n}} \mathcal{O}(\mathbf{r}, \mathbf{r}') \hat{\mathbf{n}}' \varphi_i(\mathbf{r}') \varphi_i(\mathbf{r}), \quad (57)$$

with  $\hat{\mathbf{n}} \equiv \mathbf{r}/r$  and  $\hat{\mathbf{n}}' \equiv \mathbf{r}'/r'$ . Moreover, since the Wannier wave functions are localized at the ring's sites,

$$\begin{aligned} \overleftrightarrow{T}_i &= \hat{\mathcal{R}}_i \left[ \int \int d\mathbf{r} d\mathbf{r}' \varphi_i^*(\mathbf{r}) \varphi_i^*(\mathbf{r}') \mathcal{O}(\mathbf{r}, \mathbf{r}') \varphi_i(\mathbf{r}') \varphi_i(\mathbf{r}) \right] \hat{\mathcal{R}}_i \\ &= \hat{\mathcal{R}}_i \langle ii | \mathcal{O} | ii \rangle \hat{\mathcal{R}}_i \end{aligned} \quad (58)$$

with  $\hat{\mathcal{R}}_i = \mathcal{R}_i / |\mathcal{R}_i|$ . Assuming, for simplicity, that the matrix element of  $\mathcal{O}(\mathbf{r}, \mathbf{r})$  is homogeneous, i.e.  $\langle ii | \mathcal{O} | ii \rangle = \mathcal{O}_0$  is *site independent*, and  $\mathcal{O}_0$  is a scalar of order one, we rewrite Eq.(55) as

$$\begin{aligned} w_{ijkl} \approx & - \left( \frac{mt}{\hbar} \right)^2 \mathcal{O}_0 \times \left[ (\mathcal{R}_i - \mathcal{R}_{i+1}) \cdot \hat{\mathcal{R}}_{i+1} (\mathcal{R}_{i+1} - \mathcal{R}_i) \cdot \hat{\mathcal{R}}_{i+1} \delta_{j,i+1} \delta_{l,i+1} \delta_{k,i} \right. \\ & + (\mathcal{R}_i - \mathcal{R}_{i+1}) \cdot \hat{\mathcal{R}}_{i+1} (\mathcal{R}_{i+1} - \mathcal{R}_{i+2}) \cdot \hat{\mathcal{R}}_{i+1} \delta_{j,i+1} \delta_{l,i+1} \delta_{k,i+2} \\ & + (\mathcal{R}_i - \mathcal{R}_{i-1}) \cdot \hat{\mathcal{R}}_{i-1} (\mathcal{R}_{i-1} - \mathcal{R}_{i-2}) \cdot \hat{\mathcal{R}}_{i-1} \delta_{j,i-1} \delta_{l,i-1} \delta_{k,i-2} \\ & \left. + (\mathcal{R}_i - \mathcal{R}_{i-1}) \cdot \hat{\mathcal{R}}_{i-1} (\mathcal{R}_{i-1} - \mathcal{R}_i) \cdot \hat{\mathcal{R}}_{i-1} \delta_{j,i-1} \delta_{l,i-1} \delta_{k,i} \right]. \end{aligned} \quad (59)$$

Now, we should notice that, for a  $N$ -site ring

$$\mathcal{R}_i \cdot \hat{\mathcal{R}}_i = \frac{a}{\sqrt{2(1 - \cos(2\pi/N))}}, \quad (60)$$

$$\mathcal{R}_{i\pm 1} \cdot \hat{\mathcal{R}}_i = \frac{a}{\sqrt{2(1 - \cos(2\pi/N))}} \cos\left(\frac{2\pi}{N}\right), \quad (61)$$

where  $a$  is the system's lattice spacing. Therefore, Eq.(59) simplifies to

$$w_{ijkl} \approx \left(\frac{mt}{\hbar}\right)^2 \frac{a^2 \mathcal{O}_0}{2(1 - \cos(2\pi/N))} [\delta_{j,i+1}\delta_{l,i+1}\delta_{k,i} + \delta_{j,i+1}\delta_{l,i+1}\delta_{k,i+2} + \delta_{j,i-1}\delta_{l,i-1}\delta_{k,i-2} + \delta_{j,i-1}\delta_{l,i-1}\delta_{k,i}]. \quad (62)$$

Substituting Eq.(62) into Eq.(46) we find, after a few change

$$\hat{W}_{eff} = -\frac{(tU)^2}{\Lambda^3} \frac{\mathcal{O}_0}{(1 - \cos(2\pi/N))} \sum_{j=1}^N \sum_{\sigma, \sigma'} \left[ \left( c_{j\sigma}^\dagger c_{j+1\sigma'}^\dagger c_{j\sigma'} c_{j+1\sigma} + \text{h.c.} \right) + \left( c_{j\sigma}^\dagger c_{j-1\sigma'}^\dagger c_{j-2\sigma'} c_{j-1\sigma} + \text{h.c.} \right) \right]. \quad (63)$$

The effective interaction Eq.(63) involves two types of processes, which we illustrate in Fig. 5. The first one  $\propto c_{j\sigma}^\dagger c_{j+1\sigma'}^\dagger c_{j\sigma'} c_{j+1\sigma}$  is what we called "bubble term", since it destroys an electron at the site  $j$  and creates it at the site  $j+1$ , but also destroys another electron at the same site  $j+1$  dis-

of variables,

placing it to the site  $j$ . Thus, such term restricts the electronic motion between two neighboring sites of the ring. The second term  $\propto c_{j\sigma}^\dagger c_{j-1\sigma'}^\dagger c_{j-2\sigma'} c_{j-1\sigma}$ , on the other hand, involves two neighboring sites and *favors the electron delocalization*.

Combining Eq.(63) with Eq.(2), we find the following extended Hubbard model for the  $\pi$ -electrons:

$$\hat{H} = -t \sum_{j=1}^N \sum_{\sigma} \left( c_{j\sigma}^\dagger c_{j+1\sigma} + \text{h.c.} \right) + U \sum_{j=1}^N \hat{n}_{j\uparrow} \hat{n}_{j\downarrow} - \lambda_N \left( \frac{U}{t} \right)^2 \sum_{j=1}^N \sum_{\sigma, \sigma'} \left[ \left( c_{j\sigma}^\dagger c_{j+1\sigma'}^\dagger c_{j\sigma'} c_{j+1\sigma} + \text{h.c.} \right) + \left( c_{j\sigma}^\dagger c_{j-1\sigma'}^\dagger c_{j-2\sigma'} c_{j-1\sigma} + \text{h.c.} \right) \right], \quad (64)$$

where we define the coupling constant

$$\lambda_N \equiv \frac{t^4}{\Lambda^3} \frac{\mathcal{O}_0}{(1 - \cos(2\pi/N))}. \quad (65)$$

Recall that  $\Lambda > 0$  is the energy scale of the separation between the ground and the first excited states of the  $\sigma$ -electrons, which we approximate by a constant, i.e., independent of the  $\pi$ -electrons configuration. It is important to say that it is the relation between the parameters  $t$  and  $\Lambda$  that will set the energy scale of the coupling  $\lambda_N$ . Hereafter, we set  $\mathcal{O}_0/(1 - \cos(2\pi/N)) \sim 1$  and, then, replace the coupling constant  $\lambda_N$  by simply  $\lambda \equiv t^4/\Lambda^3 < 1$ . At this point it becomes clear that  $\lambda$  is indeed the parameter that controls the validity of our generalized Born-Oppenheimer approach to this problem. If  $t/\Lambda \ll 1$ , this effective momentum-momentum coupling

is negligible and we end up with an ordinary Hubbard model where the bonding electrons are frozen at the chemical bonds and only dress the ionic potential experienced by the itinerant electrons. In other words, this new term shows that the first correction to the motion of the itinerant electrons due to the remaining electrons of the system takes place by the generation of an effective inter-electronic momentum-momentum between the former. At least for systems whose bonding electrons behave as if they were in a covalent bond, this seems to be the case.

As Eq. (64) is the central result of this work, we now investigate some of its physical consequences. In particular, we want to see what happens to the energy spectrum of the rings we studied in the beginning of this paper. In an accompanying contribution (cite) we shall address the issue of current-carrying states and the consequences of our new term to the

magnetic properties of aromatic molecules, of which benzene is a paradigmatic example. We have chosen to separate these two contributions to avoid overloading either of them, in particular the present one, with too much information.

In Fig.(3) we have presented results of the exact diagonalization of Hubbard Hamiltonians with  $N = 3, 4, 5$ , and 6 sites and the same number of  $\pi$ -electrons. For the specific case of  $N = 3$ , all the curves representing the energies as a function of  $U/t$  are explicitly shown, whereas for the other cases we have drawn only the lowest lying energy curves. Some of those energy levels are highly degenerate and can be classified according to their ability to support electric current, as we have mentioned above, but here we shall content ourselves with the effect of the new term on the energy levels of our rings.

Now, in Fig.(6), we present the same energy levels we plotted before, but including the correction proportional to  $\lambda_N$  in (64). Actually, we have considered too large a value of this coupling,  $\lambda_N = 0.1$ , in order to clearly stress the effect we are seeking. The conclusion we reach is that this term always reduces the ground state energy of the systems we have studied, but there is no systematic behavior concerning the excited states of those rings. Some of them have their ener-

gies increased whereas some other have them reduced. We also notice the possibility of level crossings between some of the excited states affected by the momentum-momentum coupling.

Although these observations are quite clear from Fig.(6), some care must be exercised when analyzing them, because, as we have already mentioned, they were obtained from a very particular - and large - value of  $\lambda_N$ . At this point a very natural question should be raised: What is the meaning of being large in this case?

In order to answer this question, we must remember that there are two dimensionless parameters in the new coupling term. One is  $\lambda_N/t$ , and the other  $(U/t)^2$ . Therefore, we cannot simply consider  $\lambda_N < t$  without saying a word about  $(U/t)^2$ . If the whole scheme of approximation we have employed is to make any sense at all, the latter must be such that the combination  $(tU)^2/\Lambda^3 \ll 1$  which implies that  $(U/t)$  cannot be much greater than one. In other words, our approximation must be reliable from small to moderate values ( $\gtrsim 1$ ) of  $(U/t)$  and, by construction,  $t/\Lambda < 1$ . This remark reinforces the idea that what our approximation really does is provide an extension of the Hubbard model which is suitable for applications to broader band correlated systems.

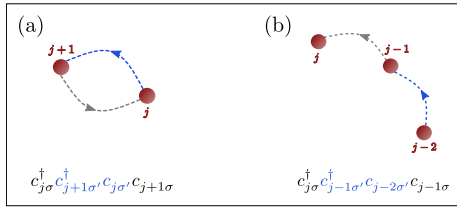


**FIG. 5. Effective interaction.** Illustration of two types of two-body processes that appear in the effective interaction Eq.(63). (a) is the "Bubble term", while (b) is the extended term that favors the electron delocalization. The Hermitian conjugates of (a) and (b) just reverse the direction of the arrows.

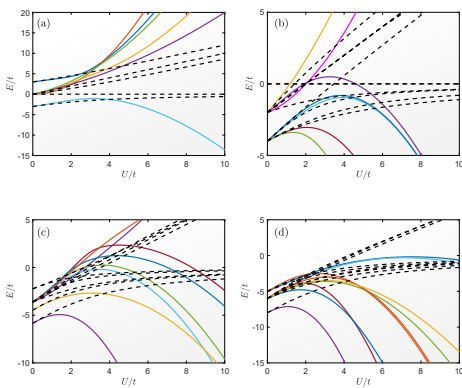


**FIG. 6. Energy spectrum of the extended Hubbard Hamiltonian.** The panels show the energy levels of Eq.(64), as a function of  $U/t$  for rings with (a)  $N = 3$  sites, (b)  $N = 4$  sites, (c)  $N = 5$  sites, and (d)  $N = 6$  sites at the half-filling regime ( $N = N_e$ ) and with  $\lambda/t = 0.1$ . In the panels (b) to (d), only a few of the low-lying energy levels are plotted. The dashed lines correspond  $\lambda = 0$ , i.e., the spectrum of the standard Hubbard model defined in Eq.(2).

#### IV. CONCLUSIONS

Although it is true that the  $\sigma$ -electrons are more localized than the  $\pi$ -electrons, they can undergo local excitations in the  $\sigma$ -bonds, which, in turn, modifies the electron charge density in the bonds, and, therefore modifies the periodic potential felt by the  $\pi$ -electrons. We show that if we allow even for virtual excitations of the  $\sigma$ -electrons to happen, they mediate an attractive momentum-momentum effective interaction between the  $\pi$ -electrons described by  $\hat{W}_{eff}$  defined in Eq.(43). The latter bears some similarities with the Biot-Savart kind of interaction derived by Pines and Bohm<sup>20-22</sup>.

Motivated by a natural energy scale separation between the  $\sigma$  and  $\pi$ -electrons, we could decouple their degrees of freedom through the employment of a wave function ansatz similar to that used in the standard Born-Oppenheimer approximation. The remaining coupling between those two kinds of electrons could then be treated within first order perturbation theory generating the above-mentioned momentum-momentum-effective interaction.

Despite there is clearly a myriad of physical problems where the consequences of the existence of this kind of term could be tested, we have decided to address only its effect on the lowest-lying energy levels of some small rings, and compare it to the results obtained by the exact diagonalization of standard Hubbard Hamiltonians as applied to the same systems. A quantitative analysis of the influence of this term on the magnetic properties of Hubbard rings and its consequences to, say - the diamagnetism of aromatic molecules-, is treated in an accompanying contribution (cite). Here we should remark that everything we have done so far relies on the results of exact diagonalization of small systems. In order to better understand our results and improve our physical

understanding of the effects of the new term we should implement other approximation methods such as, for example, mean field theory. This is something we are aiming at, and hoping to present in future contributions.

Another important question one should raise at this point is why effects of this term have never been observed so far. Well, in principle, we cannot say that they have never been observed. As we have already stressed, the importance of this term lies on a region of the parameter space at which more realistic systems should not be treated by simplified many-body models. In our particular case, we are dealing with the moderate  $U$  regime which is known to be the one to provide us with a poor physical picture when modelling realistic systems within the Hubbard scheme. The regimes  $U \ll t$  (perturbative Hückel) or  $U \gg t$  (narrow band systems) are much more appropriate to describe specific concrete situations. Therefore, we think that results arising from the extended Hubbard Hamiltonian should be compared, for example, with those obtained by the density functional theory, where one can simulate the dynamics of all kinds of electrons present in the system without drastic approximations. In this sort of comparison the effects of the new term might be buried among others we could not reach in our approximation. Nevertheless, we hope this helps us select the conditions at which the momentum-momentum coupling generates the main contribution for the observed behavior.

Finally, a few words about the generality of our result. Despite it has been obtained from a model where we tried to reincorporate the dynamics of the  $\sigma$ -electrons into that of the  $\pi$ -electrons, what is really the bottom line of our approach is the very fact that we are talking about a set of electrons which interact with another electronic system whose typical energy scale is quite different from that of the former. Whereas in the present case we have dealt with  $\sigma$  and  $\pi$ -electrons, Bohm and Pines<sup>20–22</sup> treated electron-hole pairs interacting with the long wavelength longitudinal excitations (plasmons) of the same electron gas. Although the latter authors did not recognize the suitability of the adiabatic approximation, and perturbative corrections to it, to their system, we think we have successfully done it to ours. Furthermore, there is nothing in our method which prevents us from applying it to more

general systems once we identify the existence of the basic ingredients necessary for the implementation of the generalized Born- Oppenheimer approximation, and consequently the generation of an effective momentum-momentum interaction between the components of the electronic system of interest. It should be, at least instructive, to study the possible effects of this term in 2D electronic systems such as graphene sheets or Cu-O planes in high- $T_c$  materials.

## ACKNOWLEDGMENTS

We acknowledge São Paulo Research Foundation (FAPESP) and Conselho Nacional de Desenvolvimento Científico e Tecnológico (CNPq) for the financial support. TTV and GMM were supported by FAPESP under the projects 2015/21349-7 and 2016/13517-0, respectively, whereas AOC was supported by CNPq under the project 302420/2015-0.

## Appendix: Matrix element of $\mathbf{P}$ in the site basis

The first thing we should note is that  $\mathbf{V} \equiv \mathbf{P}/m$ , where  $m$  denotes the electron mass, is simply the electron *velocity operator*, which is related to the system's single-particle Hamiltonian through the commutator

$$\mathbf{V} = \frac{1}{i\hbar} [\mathbf{R}, h] . \quad (\text{A.1})$$

Here, we denote by  $\mathbf{R}$  the electron position operator and we recall that the single particle Hamiltonian, in the coordinate representation, is given by

$$h(\mathbf{r}) \equiv \frac{\mathbf{P}^2}{2m} + V_c(\mathbf{r}) = -\frac{\hbar^2}{2m} \nabla^2 + V_c(\mathbf{r}) . \quad (\text{A.2})$$

Evaluating the matrix element of Eq.(A.1) in the single-particle Wannier wave functions  $\varphi_j(\mathbf{r}) = \langle \mathbf{r} | j \rangle$ , we obtain

$$\left\langle j_1 \left| \frac{1}{i\hbar} [\mathbf{R}, h] \right| j_2 \right\rangle = \frac{1}{m} \langle j_1 | \mathbf{P} | j_2 \rangle = \frac{1}{i\hbar} (\langle j_1 | \mathbf{R} h | j_2 \rangle - \langle j_1 | h \mathbf{R} | j_2 \rangle) . \quad (\text{A.3})$$

Now, inserting the closure relation

$$\mathbb{1} = \sum_{j=1}^N |j\rangle \langle j| \quad (\text{A.4})$$

between the  $\mathbf{R}$  and  $h$  operators on the right-hand side of Eq.(A.3) and approximating the position matrix elements as

$$\langle j_1 | \mathbf{R} | j_2 \rangle \approx \mathcal{R}_{j_2} \langle j_1 | j_2 \rangle = \mathcal{R}_{j_2} \delta_{j_1, j_2} , \quad (\text{A.5})$$

which is justified by the fact that the Wannier function  $\varphi_j(\mathbf{r})$  is localized about the  $j$ -th site of the ring, whose position we denote by  $\mathcal{R}_j$ , we readily find

$$\frac{1}{m} \langle j_1 | \mathbf{P} | j_2 \rangle = \frac{1}{i\hbar} (\mathcal{R}_{j_1} - \mathcal{R}_{j_2}) \langle j_1 | h | j_2 \rangle . \quad (\text{A.6})$$

Finally, recalling that  $\langle j_1 | h | j_2 \rangle = t_{j_1, j_2}$  gives the hopping between the sites  $j_1$  and  $j_2$ , which, in the nearest-neighbor

approximation, simplifies to

$$\langle j_1 | h | j_2 \rangle \approx -t\delta_{j_2,j_1\pm 1}, \quad (\text{A.7})$$

we obtain Eq.(54):

$$\langle j_1 | \mathbf{P} | j_2 \rangle = -\frac{mt}{i\hbar} (\mathcal{R}_{j_1} - \mathcal{R}_{j_2}) \delta_{j_2,j_1\pm 1}. \quad (\text{A.8})$$

- <sup>\*</sup> Present address: Ames Laboratory, Ames, Iowa 50011, USA
- <sup>†</sup> Present address: Department of Physics, City College, City University of New York, New York, NY 10031, USA
- <sup>1</sup> L. D. Landau, Sov. Phys. , JETP, **3**, 920 (1957).
- <sup>2</sup> D. Pines and P. Nozières, *The Theory of Quantum Liquids* (W. A. Benjamin, Inc.) (1966).
- <sup>3</sup> L. D. Landau, Sov. Phys. , JETP, **8**, 70 (1959).
- <sup>4</sup> N. W. Ashcroft and N. D. Mermin, *Solid State Physics* (Holt, Reinhart and Winston) (1976).
- <sup>5</sup> A. L. Fetter, J. D. Walecka *Quantum Theory of Many-Particle Systems* (McGraw-Hill, San Francisco) (1971).
- <sup>6</sup> G. D. Mahan *Many-Particle Physics* (Plenum Press, New York) (1981).
- <sup>7</sup> L. N. Cooper, Phys. Rev., **104**, 1189 (1956).
- <sup>8</sup> J. Bardeen, L. N. Cooper, and J. R. Schrieffer, Phys. Rev., **108**, 1175 (1957).
- <sup>9</sup> P. Coleman *Introduction to Many-Body Physics* (Cambridge University Press) (2015)

- <sup>10</sup> S. K. Maiti, Sol. State. Commun. **150**, 2212 (2010).
- <sup>11</sup> J. Hubbard, Proc. R. Soc. A **276**, 238 (1963).
- <sup>12</sup> S. Doniach and E. H. Sondheimer *Green's Functions for Solid State Physicists* (Imperial College Press) (1998).
- <sup>13</sup> E. H. Lieb and F. Y. Wu, Phys. Rev. Letters **20** 1445 (1968).
- <sup>14</sup> K. Kaiser et al., Science 10.1126/science.aay1914 (2019).
- <sup>15</sup> A. J. Heeger, Rev. Mod. Phys. **73** 681 (2001).
- <sup>16</sup> C. Cohen-Tannoudji, B. Diu and F. Laloe *Quantum Mechanics*, Vol.1 (New York, NY; Paris: John Wiley) (2005).
- <sup>17</sup> G. Baym *Lectures on Quantum Mechanics* (W. A. Benjamin, Massachusetts) (1973).
- <sup>18</sup> T. V. Trevisan, Ph.D. Thesis (UNICAMP) (2019)
- <sup>19</sup> T. V. Trevisan, G. M. Monteiro and A. O. Caldeira, Phys. Rev. Letters.
- <sup>20</sup> D. Bohm and D. Pines, Phys. Rev. **82**, 625 (1951).
- <sup>21</sup> D. Bohm and D. Pines, Phys. Rev. **85**, 338 (1952).
- <sup>22</sup> D. Bohm and D. Pines, Phys. Rev. **92**, 609 (1953).
- <sup>23</sup> W. D. Jackson *Classical Electrodynamics* (John Wiley and Sons, Inc.) (1962).